

## InSb arrays for IRAC (InfraRed Array Camera) on SIRTf (Space Infrared Telescope Facility)

J.L. Pipher<sup>\*a</sup>, W.J. Forrest<sup>a</sup>, W.J. Glaccum<sup>a</sup>, R.G. Benson<sup>a</sup>, D.J. Krebs<sup>b</sup>, M.D. Jhabvala<sup>b</sup>, J.P. Rosbeck<sup>c</sup>, N.A. Lum<sup>c</sup>, W.Y. Lum<sup>c</sup>, J.D. Garnett<sup>c,d</sup>, A.W. Hoffman<sup>c</sup>, G. Domingo<sup>c,e</sup>, G.M. Cushman<sup>f</sup>, D.A. Rapchun<sup>f</sup>

<sup>a</sup>Dept. of Physics and Astronomy, University of Rochester, Rochester NY 14627

<sup>b</sup>NASA Goddard Space Flight Center, Greenbelt MD 20771

<sup>c</sup>Raytheon Infrared Operations, Goleta CA 93117

<sup>d</sup>Rockwell Science Center, Thousand Oaks CA 91360

<sup>e</sup>Jet Propulsion Lab, Pasadena CA 91109

<sup>f</sup>Raytheon Technical Services Company, Greenbelt MD 20770

### ABSTRACT

SIRTf requires detector arrays with extremely high sensitivity, limited only by the background irradiance. Especially critical is the near infrared spectral region around 3  $\mu\text{m}$ , where the detector current due to the zodiacal background is a minimum. IRAC has two near infrared detector channels centered at 3.6 and 4.5  $\mu\text{m}$ . We have developed InSb arrays for these channels that operate with dark currents of  $<0.2 \text{ e}^-/\text{s}$  and multiply-sampled noise of  $\sim 7 \text{ e}^-$  at 200s exposure. With these specifications the zodiacal background limited requirement has been easily met. In addition, the detective quantum efficiency (DQE) of the InSb devices exceeds 90% over the IRAC wavelength range, they are radiation hard, and they exhibit excellent photometric accuracy and stability. Residual images have been minimized. The Raytheon 256 x 256 InSb arrays incorporate a specially developed (for SIRTf) multiplexer and high-grade InSb material.

**Keywords:** InSb, Detector Arrays, Infrared, Space Mission, SIRTf

### 1. INTRODUCTION

Extremely low space background emission levels near 3  $\mu\text{m}$ , where zodiacal dust emission and scattering reaches a minimum, place stringent requirements on the performance of channel 1 (centered at 3.6  $\mu\text{m}$ ) and channel 2 (centered at 4.5  $\mu\text{m}$ ) InSb arrays for SIRTf's four-channel InfraRed Array Camera IRAC. The dark current/pixel of the devices must be less than 1  $\text{e}^-/\text{s}$  and the combined noise sources less than 10  $\text{e}^-/\text{pixel}$  in order for these camera channels to be natural background-limited. Other SIRTf requirements dictate high quantum efficiency, minimal image latency, high stability, excellent photometric accuracy, radiation hardness, and no anomalous behaviors. The University of Rochester (UR) members of the IRAC team worked with Raytheon Infrared Operations (RIO, formerly SBRC) to develop both the detector material and the multiplexers for operation of the focal planes at 15K. Much of this work, including the development effort, has been reported previously<sup>1,2,3</sup> and only recent developments and results will be cited here. In a nutshell, the InSb focal planes selected for IRAC meet the noise and dark current specifications by a considerable margin. All the flight devices consist of low-doped, high purity InSb diodes bump-bonded to a CRC744 multiplexer. The InSb thickness is designed to be  $7 \pm 1 \mu\text{m}$ . Testing in the UR lab was conducted on a sensor chip assembly (SCA) – an InSb detector array mounted to a 68-pin leadless carrier which mated to a socket mounted on a specially designed fanout board, where thermal control was made through the unused pins connected to a thermal metal ground plane on the fanout board.

GSFC (Goddard Space Flight Center) and UR tested candidate flight SCAs: at least one device was tested in common so that a suitable intercomparison of the two labs' work could be made. The clocking developed by Forrest at the University of Rochester (specially designed so that a row is always enabled, and allowing operation of the device even if  $V_{\text{clamp}}$  is inoperative) was utilized at both labs, and on the flight instrument IRAC. In addition, it allows fast sub-array readout, a mode which is being used on IRAC.

GSFC designed the IRAC FPA (focal plane assembly) to replace the leadless chip carrier, and it is described below. Most FPA tests were conducted at GSFC, as were tests of IRAC (described in a companion paper<sup>4</sup> in this session of this

\* Correspondence: E-mail: [jlipher@pas.rochester.edu](mailto:jlipher@pas.rochester.edu); Telephone: 716 275 4402; Fax: 716 275 8527

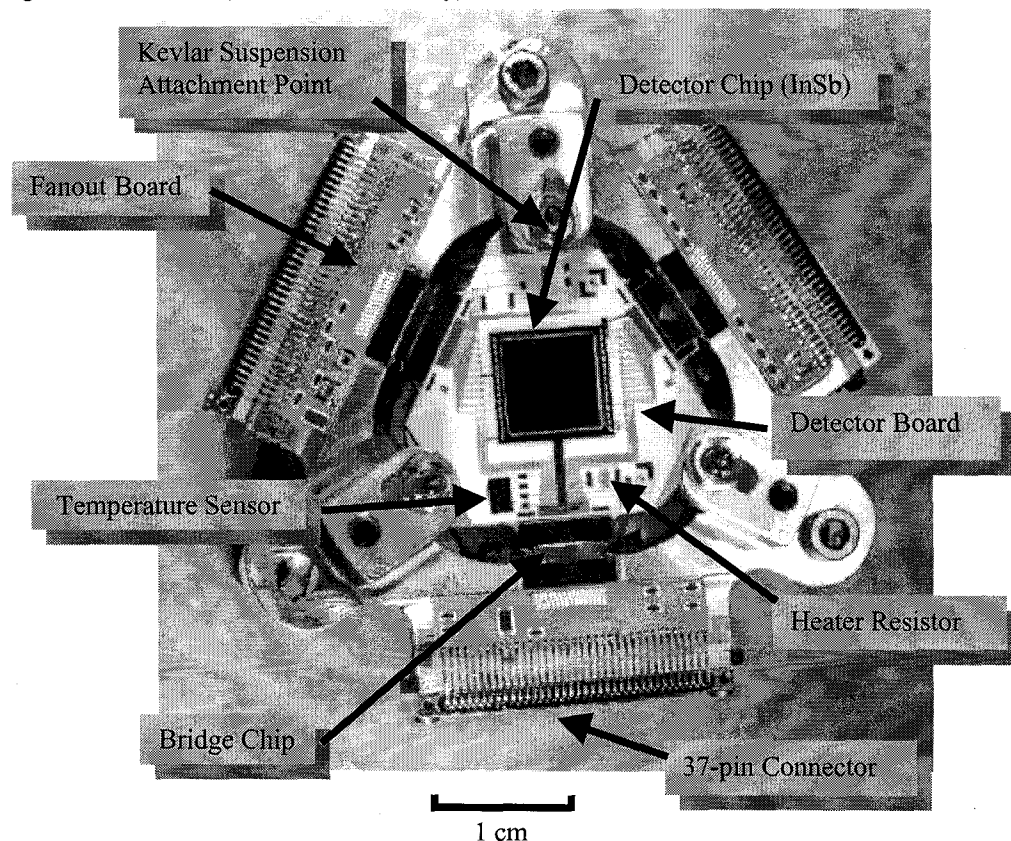
## 2. DESCRIPTION OF TESTING OF FLIGHT CANDIDATE SCAS

Prior to delivery, flight candidate SCAs were measured at Raytheon (formerly Santa Barbara Research Center) for quantum efficiency, read noise, multiplexer gain and power dissipation. Following delivery to either GSFC or UR, the detectors were subjected to a more extensive series of tests, including but not limited to quantum efficiency, dark current, read noise, node capacitance, multiplexer gain, well depth, image latency, and power dissipation. The majority of testing of the InSb SCAs was accomplished at the University of Rochester. Some SCA testing of the InSb devices was conducted at NASA GSFC and cross-calibration of equipment at the two facilities was maintained by means of common tests by both labs of one device. SCAs that met the flight requirements as specified by the project (outlined by Fazio *et al.*<sup>5</sup>), were returned to Raytheon (RIO) for de-bonding from the 68-pin leadless chip carrier and bonding to the ceramic flight focal plane boards developed by GSFC. The focal plane boards were then returned to GSFC for mounting into FPAs – focal plane assemblies, and testing (see below).

## 3. IRAC FOCAL PLANE ASSEMBLY DESCRIPTION

Figure 1 shows the IRAC Focal Plane Assembly (FPA). The FPA consists of the multiplexed detector array (InSb in channels 1 and 2) mounted on a ceramic focal plane board, an Invar mount body, six Kevlar straps for focal plane board suspension, bridge chips, three hybrid fanout boards, and three single-row electrical connectors. In addition to the detector array, the focal plane board has two heater resistors, two silicon diode temperature sensors, two thin-film-ceramic-oxynitride temperature sensors, seven filter capacitors for the array biases, and a series protection resistor for the detector bias. The three fanout boards, which are multi-layer hybrid circuit boards fabricated by Johns Hopkins Applied Physics Laboratory, contain static protection resistors.

Figure 1. IRAC FPA (Focal Plane Assembly)



In order to limit the thermal load of the focal planes, it is a requirement that the each IRAC/SIRTf FPA dissipates less than 1.0 mW of power. The design approach is to provide sufficient thermal isolation between the focal planes and the instrument housing such that the detectors self-heat to a significant fraction of their operating temperature. The InSb FPAs nominally operate at 15.0 K, approximately 13 K above the base temperature of the instrument enclosure. These conditions imply a minimum average thermal resistance of 13,000 degrees Kelvin per watt between 2.1K and 15K. This high level of thermal isolation is achieved by using Kevlar suspension for mechanical control of the focal plane board and silicon bridge chips for electrical connectivity<sup>6</sup>. The Kevlar suspension provides an extremely rigid and robust mechanical interface, and the silicon bridge chips provide densely packed electrical connections. Using three bridge chips per focal plane assembly, a total of 90 electrical wires, each with approximately 8 ohms of electrical resistance are available to operate and monitor each focal plane. For the InSb arrays, we employed three aluminum wire bonds to adjust the thermal isolation such that the focal planes would heat to approximately 10K due to the detector power dissipation alone. Additional heating, provided by the heater resistors, provided excellent control of the focal plane temperature. A temperature stability to approximately 0.001K was demonstrated utilizing active temperature control.

A performance test, similar to the one previously performed on the SCA, was performed following FPA assembly. There was no significant or systematic difference in the performance of the detector arrays in FPA mounts versus their performance in 68-pin leadless chip carriers (LCC). The detector tests were repeated after vibration and thermal/vacuum environmental test; the InSb FPAs still exhibit nominal behavior (see below).

#### 4. BASIC TEST RESULTS

Table 1 shows basic test results for the two InSb arrays which were selected for the IRAC instrument. There was generally good agreement between lab tests performed on the FPAs and tests performed on the leadless chip carrier-mounted devices, the SCAs. The unphysical DQEs quoted (somewhat greater than 100%) are attributed to uncertainties in the radiometry and node capacitance. In a test of a SIRTf-type array at 0.56  $\mu\text{m}$ , the DQE was measured to 2% precision by comparison with a calibrated detector: the DQE was 95%. These measurements were obtained on a SIRTf array with a single layer AR coating (optimized at 3.5  $\mu\text{m}$ ): at the interference peaks, the response was approximately flat from 0.56  $\mu\text{m}$  to longer wavelengths.

Table 1. Results of basic detector tests on the two InSb IRAC flight focal planes

Device	Mount	Test Location	Mux Gain	Well Size (e <sup>-</sup> )	DQE (%) & $\lambda$ ( $\mu\text{m}$ )	Noise (e <sup>-</sup> ) Fowler16 200s exposure	Pixel Dark Current (e <sup>-</sup> /s)	Operability (%)
Channel 1	LCC	UR	0.866	142,000	106(3.3)	8.3	0.1	99.97
#48534	FPA	GSFC	0.892	157,600	127(3.5)	8.3	0.5	99.97
Channel 2	LCC	UR	0.869	143,000	96(3.3)	7.3	0.2	99.84 <sup>#</sup>
#48975	FPA	GSFC	0.888	143,500	129(4.4)	9.1	0.1	99.90

<sup>#</sup> This low operability was due to surface contamination, removed at SBRC during re-mounting.

These focal planes met or exceeded the instrument requirements in all categories of detector performance. In order to arrive at an operability measurement, we developed bad pixel masks for DQE, read noise, well depth, and dark current. We then performed an "or" operation on three or four of those bad pixel masks to arrive at an overall bad pixel frame. The requirement was that there be no more than one area per 250 x 250 sub-array with more than four adjacent bad pixels and that the overall fraction of bad pixels be less than 0.5 percent. The band 1 and 2 arrays satisfied that requirement.

It should be noted that the noise performance of the channel 1 and 2 arrays in IRAC is comparable to that achieved in the two test labs. The total noise is the quadrature sum of the detector/mux read noise, the Poisson noise in any dark charge collected, and the electronic system noise. Sequences of 200s Fowler 32 dark images in IRAC led to rms pixel noise of 7.4 and 7.2 e<sup>-</sup> respectively for channels 1 and 2. Fowler 32 is an improvement over Fowler 16 (see reference 3, Wu *et al.*, for elaboration of Fowler sampling as well as a discussion of noise as a function of Fowler number) and these values are

comparable to the Fowler 16 noise of  $8.3\text{ e}^-$  quoted for channel 1 (Table 1). The system stability of IRAC is better than routinely achieved in the UR test labs, and is within the noise (read noise and noise in the dark charge): thus the IRAC noise figures realized are better than shown in the table for lab testing.

## 5. OTHER MEASUREMENTS

In addition to the basic detector performance parameters tabulated above, there are a variety of additional considerations (category 3 goals) which flight detector arrays are planned to satisfy. Radiation hardness, minimal image latency, stability, optical and electronic cross-talk immunity comprise some of these considerations. In addition, use of these devices in low background situations is discussed.

### 5.1 Image Latency

One of the category 3 image latency goals on IRAC arrays is that for a source flux per pixel of  $2500\text{ e}^-/\text{s}$ , 20s exposure ( $50,000\text{ e}^-$  fluence), 0s (200s) delay, the latent image fluence per pixel following cessation of exposure (20s exposure) shall be less than  $10\text{ e}^-$  ( $1\text{ e}^-$ ). UR laboratory measurements of the residual images of an extended source were made, and formed the partial basis for flight detector array selection. Channel 1 did not meet the IRAC goal: it exhibited 1<sup>st</sup> latent fluences of  $72\text{ e}^-/\text{pixel}$  ( $3\text{ e}^-/\text{pixel}$ ), while Channel 2 was much closer to the goal: it exhibited  $25\text{ e}^-/\text{pixel}$  ( $1\text{ e}^-/\text{pixel}$ ). These tests were at 450 mV applied reverse bias. Residual image testing in IRAC at GSFC at flight 500 mV applied reverse bias was conducted for both an extended source and a point source.

Reducing image latency in InSb arrays is addressed in the companion paper in session 3 of this conference (4131) by Benson *et al.*<sup>7</sup>. As discussed there, increasing the reverse bias across the diodes diminishes the residual image strength. There was a practical limitation imposed by the bias-dependent effect of increased multiplexer bleed (see below), so we settled on a compromise reverse bias of 500 mV for both channels 1 and 2. While this will provide some improvement over UR lab testing ( $\sim 25\%$ ), it is not as much improvement as would be obtained at an applied reverse bias of 750 mV.

Recent tests of image latency in IRAC (with channels 1 and 2 biased at 500 mV) led to the following results. After a 100s delay following extended source exposure ( $\sim 50,000\text{ e}^-$  source fluence),  $< 0.005\%$  or  $< 2.5\text{ e}^-$  residual image/pixel was seen in both channels 1 and 2. For a central point source fluence of  $126,000\text{ e}^-$  in band 2 (larger source flux), following a 100s delay, the residual image was 0.028% of this larger source fluence, or  $35\text{ e}^-$ . It is well known that latent image strength depends on both flux and fluence (each  $2.5\times$  specification above), but the point source tests here were not controlled to the category 3 fluxes and fluences given above.

### 5.2 Radiation Hardness

SCA 40544, a flight-like InSb array bonded to a CRC744 multiplexer, was exposed to  $\gamma$ -irradiation (660 keV Cs137) and the following week to proton fluxes from 70 and 110 MeV beams at the Harvard Cyclotron. These energies were degraded to 20 and 80 MeV respectively by the time the beams hit the detector array at an angle of  $77^\circ$  to detector normal. Fluxes ranging from  $100 - 5 \times 10^5\text{ protons/cm}^2\text{-s}$  irradiated the array for varying exposure times, up to a total dose of  $2.2\text{ krad-Si}$ . The effects of multitudes of hits at lower fluxes generally disappeared by the next frame. Pixel hits occurred singly occasionally, but more often in clumps of  $\sim 4$  pixels. At high flux levels, after 1 hour delay, the dark current had declined to  $\sim 1\text{ e}^-/\text{s}$  and the remaining hot pixels  $< 3.9\%$ . Ninety minutes following final exposure, there were  $< 1\%$  hot pixels remaining. It should be noted that the enhanced 'dark' current was caused by photo-emission from heating of the filter wheel via proton bombardment. In addition, our dewar acted as the beam-stop, and it became radioactive: many of the observed "hot pixels" were from hits by these secondaries. Neither the DQE nor the linearity of the detector were affected.

### 5.3 Stability

Long term radiometric stability of flight-like array SCA 41944 was measured at UR (200s integration,  $2.3\text{ }\mu\text{m}$  radiation, 20% full wells [ $20,000\text{ e}^-/\text{pixel}$  fluence]). The array was staring out the dewar window at a black cloth whose temperature was monitored. During the 8 hours the temperature of the black cloth was stable, the {standard deviation/mean} was 0.12%, satisfying the IRAC goal.

Electronic instability (basically instability in the detector bias or some other sensitive bias) can render determination of absolute level difficult, especially at low or nil signal levels. Our goal is to measure a zero signal-level condition with a stability better than the noise specification ( $10\text{ e}^-$ ) or even better, within the lower measured noise of the system. In the absence of reference detectors to monitor and correct for these instabilities, careful design by GSFC of the biases, of the

temperature control of the FPA, and the preamplifiers, led to the desired goal for IRAC being achieved. RMS deviations of the zero point in channels 1 and 2 measured in IRAC with long sequences of 30s Fowler 16 frames, is  $< 2 e^-$ .

#### 5.4 Optical and Electronic Cross-talk; Mux Bleed

Electronic cross-talk can be detected four pixels over on a row (every fourth pixel uses the same output amplifier). As discussed in Wu *et al.*, through use of hot pixels, the devices easily pass the  $< 1\%$  IRAC specification.

One component of electronic cross-talk derives from the limited slew rate of the mux output FET driving a capacitive line. We distinguish this from mux bleed (a glow which continues from a hot pixel most of a row at not greatly reduced intensity) even though both fall into the general electronic cross-talk category.

Mux bleed was minimized by multiplexer lot selection. Although the cause is not fully understood, mux bleed originates in freezeout at 15K within the silicon. The resultant glow falls off as a slow exponential, but is well below the IRAC electronic cross-talk specification, and can be removed in post-processing.

Optical cross-talk originates within the InSb detectors, and is wholly the result of diffusion<sup>8</sup>. A photon (limited by cold band-pass filters to the channel 1 and 2 wavelength passbands) incident on the back-surface of the InSb is absorbed within a few microns of the surface. The hole of the electron-hole pair produced diffuses to the diode junction where it is collected. Since the vertical distance over which diffusion takes place can be as large as 3-4  $\mu\text{m}$ , there is the possibility of adjacent pixel diodes gathering the charge corresponding to an incident photon. In an analysis of optical quality of IRAC, there was evidence for diffusion seen, at about the level expected from spot-scan tests of a flight-like InSb detector array conducted at  $\lambda = 0.6 \mu\text{m}$  - where the vertical distance over which diffusion takes place is closer to 4.5  $\mu\text{m}$ .

#### 5.5 Magnetic Field Susceptibility

SIRTF-like arrays were tested in magnetic (B) fields of 27.6 gauss in 6 directions, parallel to the principal axes of a non - illuminated array. The mean difference between B-on and B-off, Fowler 64, 200s integrations, is considerably less than  $5 e^-$ .

SIRTF-like InSb detector arrays have been used for several years in astronomical observations. Even at J-band (centered at 1.23  $\mu\text{m}$ ), the OH sky brightness is considerably higher than the minimum zodiacal brightness encountered in space. We have used these arrays with 2% circular variable filter wheels in series with a Fabry Perot interferometer<sup>9,10,11</sup> of resolution  $R = 800$  which limits the background, and have successfully obtained well-calibrated, repeatable measurements with a background level incident on the detector of 2.3  $e^-/\text{s}$ , less than the minimum background encountered by IRAC. These observations comprise proof-of-concept low background measurements with IRAC arrays.

#### 5.6 Vibration Tests

In order to verify the capability of the FPAs to survive launch conditions, we performed vibration tests in various configurations and at various temperatures. In one set of tests, two FPAs were vibrated to approximately 6 G rms in two axes and 10.6 G rms in the third axis at 77K. The vibration limits for those tests were set by the capabilities of the vibration test dewar, not by any other considerations. We also performed room temperature vibration tests on a flight-candidate FPA to 16.1 G rms. In addition to detailed inspection of mechanical integrity, detector characterization was performed before and after each vibration. No failure or damage occurred as a result of vibration. In addition, the four flight focal planes have successfully completed vibration at the instrument level (6 G rms, 20-2000 Hz, 218.1 lbs rms force limit) with no degradation in instrument performance.

## 6. IRAC STATUS

The IRAC instrument is just completing its test cycle at GSFC prior to delivery to Ball Bros., and integration into the MIC (multiple instrument chamber). SIRTF is scheduled to launch in December 2001, and to begin science observations early in 2002.

## REFERENCES

1. J. L. Pipher, W.J. Forrest, and J. Wu, *SPIE Infrared Detectors Instrumentation* **2475**, pp. 428 ,1995.
2. J.D. Garnett and W.J. Forrest, "Multiply sampled read limited and background limited noise performance", *SPIE Infrared Detectors Instrumentation* **1946**, pp. 395-404 ,1993.

3. J. Wu, W.J. Forrest, J.L. Pipher, N. Lum and A. Hoffman, "Development of infrared focal plane arrays for space", *Review of Scientific Instruments* **68**, pp. 3566-3578, 1997.
4. J. L. Hora, G.G. Fazio, S.P. Willner, M.L.N. Ashby, J. Huang, S.T. Megeath, J.R. Stauffer, E.V. Tollestrup, Z. Wang, J.L. Pipher, W.J. Forrest, C.R. McCreight, W.F. Hoffman, P. Eisenhardt, J.A. Surace, S.H. Moseley, K.P. Stewart, F.D. Robinson, "Calibration and performance of the Infrared Array Camera (IRAC)" this meeting, 2000.
5. G.G. Fazio, J.L. Hora, S.P. Willner, J.R. Stauffer, M.L.N. Ashby, Z. Wang, E.V. Tollestrup, J.L. Pipher, W.J. Forrest, C. McCreight, S.H. Moseley, W.F. Hoffman, P. Eisenhardt, E. Wright, "The Infrared Array Camera (IRAC) for the Space Infrared Telescope Facility (SIRTF)" *SPIE Infrared Astronomical Instrumentation* **3354**, pp.1024-1031, 1998.
6. C.A. Allen, S.H. Moseley, D.S. Schwinger, A. Elvin, "Low Thermal Conductance Silicon Bridges Fabricated by MEMS Processing Techniques for Cryogenic Electrical Interconnects", *Nanospace 98, The International Conference on Integrated Nano/Microtechnology for Space Applications*, Houston TX, November, 1998.
7. R.G. Benson, W.J. Forrest, J.L. Pipher, W. Glaccum, S.L. Solomon, "Spatial Distributions of Hole Traps and Image Latency in InSb Focal Plane Arrays", this meeting, 2000.
8. M. Davis, M. Greiner, J. Sanders, J. Wimmers, "Resolution issues in InSb focal plane array system design" *SPIE Conference on Infrared Detectors and Focal Plane Arrays V*, **3379**, pp. 288-299, 1998.
9. J.A. Goetz, J.L. Pipher, W.J. Forrest, D.M. Watson, S.N. Raines, C.E. Woodward, M.A. Greenhouse, H.A. Smith, V.A. Hughes, and J. Fischer, "Cepheus A East: Unravelling the Mysteries", *ApJ* **504**, pp. 359-374, 1998.
10. J.D. Bloomer, D.M. Watson, J.L. Pipher, W.J. Forrest, B. Ali, M.A. Greenhouse, S. Satyapal, H.A. Smith, J. Fischer, C.E. Woodward, "A Near-Infrared Study of NGC 7538 IRS 1, 2, and 3", *ApJ* **506**, pp. 727-741, 1998.
11. S.N. Raines, D.M. Watson, J.L. Pipher, W.J. Forrest, M.A. Greenhouse, S. Satyapal, C.E. Woodward, H.A. Smith, J. Fischer, J.A. Goetz, A. Frank, "Large Proper-Motion Infrared [FeII] Emission-Line Features in GGD 37", *ApJ* **528**, pp. L115-L118, 2000.